Published in final edited form as:
Eur J Neurosci. 2011 February ; 33(3): 409–420. doi:10.1111/j.1460-9568.2010.07547.x.

Somatosensory inputs modify auditory spike timing in dorsal cochlear nucleus principal cells

Seth D Koehler[1,3], **Shashwati Pradhan**[1], **Paul B Manis**[4], and **Susan E Shore**[1,2]

[1] Kresge Hearing Research Institute, Department of Otolaryngology, University of Michigan Medical School, Ann Arbor, MI 48109

[2] Department of Molecular and Integrative Physiology, University of Michigan Medical School, Ann Arbor, MI 48109

[3] Department of Biomedical Engineering, University of Michigan, Ann Arbor, MI 48109

[4] Department of Otolaryngology/Head and Neck Surgery and Department of Cell and Molecular Physiology, The University of North Carolina at Chapel Hill, Chapel Hill, NC 27599-7070

Abstract

In addition to auditory inputs, dorsal cochlear nucleus (DCN) pyramidal cells in the guinea pig receive and respond to somatosensory inputs and perform multisensory integration. DCN pyramidal cells respond to sounds with characteristic spike-timing patterns that are partially controlled by rapidly inactivating potassium conductances. Deactivating these conductances can modify both spike rate and spike timing of responses to sound. Somatosensory pathways are known to modify response rates to subsequent acoustic stimuli, but their effect on spike timing is unknown. Here, we demonstrate that preceding tonal stimulation with spinal trigeminal nucleus (Sp5) stimulation significantly alters the first spike latency, the first interspike interval, and the average discharge regularity of firing evoked by the tone. These effects occur whether the neuron is excited or inhibited by Sp5 stimulation alone. Our results demonstrate that multisensory integration in DCN alters spike-timing representations of acoustic stimuli in pyramidal cells. These changes likely occur through synaptic modulation of intrinsic excitability or synaptic inhibition.

Keywords

Guinea Pig; Cochlear Nucleus; Auditory; Trigeminal; Somatosensory; Multisensory; Spike Timing

Introduction

The principal output cells of the dorsal cochlear nucleus (DCN), the pyramidal cells, are activated by sound through auditory nerve inputs onto their basal dendrites (Manis and Brownell 1983; Stabler, Palmer et al. 1996). However, these cells also receive somatosensory input from dorsal column and trigeminal brainstem nuclei (Kirzinger and Jurgens 1991; Wright and Ryugo 1996; Luthe, Hausler et al. 2000; Zhou and Shore 2004; Haenggeli, Pongstaporn et al. 2005). These excitatory projections terminate initially on CN granule cells (Zhou, Nannapaneni et al. 2007) whose axons then activate the apical dendrites of the pyramidal cells (Figure 1). The first studies to demonstrate responses of pyramidal

sushore@umich.edu, Telephone: (734) 647-2116, Fax: (734) 764-0014.

cells to the somatosensory system (Saade, Frangieh et al. 1989; Davis, Miller et al. 1996; Kanold and Young 2001) showed that these cells could be excited or inhibited by stimulating brainstem somatosensory nuclei. Later studies showed that bimodal stimulation with sound and somatosensory stimulation could enhance or suppress the firing rates of pyramidal cells to the sound stimulus (Shore 2005; Shore, Koehler et al. 2008) demonstrating that these cells are capable of multiplicative multisensory integration (Stein and Meredith 1990; Stein and Meredith 1993; Populin and Yin 2002; Meredith, Keniston et al. 2006). While multisensory integration is usually analyzed using average spike rate, more recent reports show that multisensory integration can also be represented by alterations of spike timing (Zahar, Reches et al. 2009).

The spike timing of pyramidal cells is influenced by the membrane potential prior to depolarization (Manis 1990; Kanold and Manis 1999). *In vitro* studies show that prior hyperpolarization can delay first spike latencies (FSLs) and increase the first interspike intervals (FISI) (Manis 1990; Kanold and Manis 2005), as well as alter firing precision (Street and Manis 2007), suggesting that brief perturbations across sensory domains, through multisensory integration, could influence spike timing. Altering spike-timing of pyramidal cells by somatosensory inputs could change the way these cells encode sound and influence the representation of sound-location information (Young, Spirou et al. 1992; May 2000; Oertel and Young 2004), as well as filtering self-generated sounds (Bell, Bodznick et al. 1997; Oertel and Young 2004). These tasks can utilize contextual somatosensory information regarding face or vocal muscle movement, pinnae and/or head position time-locked to an auditory stimulus. Consequently, we investigated the effects of auditory-somatosensory integration on spike-timing of responses to sound in pyramidal cells. We predicted that *in vivo* activation of granule cell inputs to pyramidal cells by trigeminal nucleus (Sp5) stimulation would change pyramidal cell characteristic temporal responses by delaying FSLs and FISIs and changing firing regularity and precision.

Materials and Methods

Surgical Preparation

Experiments were performed on 7 mature, female, pigmented guinea pigs (250–350 g, Elm Hill). All procedures were approved by the University of Michigan Committee on the Use and Care of Animals (UCUCA). Animals were anesthetized with ketamine (40 mg/kg) and xylazine (10 mg/kg) and held in a stereotaxic device (Kopf) with hollow ear bars for the delivery of sounds. Rectal temperature was monitored and maintained at 38 ± 0.5°C with a thermostatically-controlled heating pad. Supplemental anesthesia (0.25–0.5X initial dose) was given approximately hourly, after performing a digital pinch test to elicit paw withdrawal. Unit thresholds to broadband noise were monitored throughout the experiment to assess the physiological condition of the animals. The bone overlying the cerebellum and posterior occipital cortex was removed and a small amount of cerebellum was aspirated to reveal the surface of DCN.

Acoustic Stimulation

Acoustic stimuli were 100 ms broadband noise or 50 ms tone bursts (1.5 ms rise/fall times) presented at different levels to assess neural thresholds, BFs, latencies and rate-level functions. Stimuli were delivered to the ears with Beyer dynamic earphones (DT-48) coupled to the hollow ear bars using TDT system III hardware for digital-to-analog conversion and analog attenuation. Digital signals were generated and delivered to the TDT hardware by a Pentium PC using a custom MATLAB software package. Stimuli were generated using a sampling rate of 50 kHz with 16-bit resolution. Tones were calibrated using a ¼ inch condenser microphone (Bruel & Kjaer, Mic:4136, Preamp:2619, Power

Supply:2804) coupled to the ear bar with a 0.2 ml tube. The microphone output was measured using custom MATLAB software. Noise was calibrated with the ¼ inch microphone and coupler attached to a sound level meter set to measure the bandwidth of interest (200 Hz–20 kHz for broad band noise). Equalization to correct for the system response was performed in the frequency domain using digital filters implemented in TDT hardware. The stimulus variable sequences were generated in pseudorandom order from within MATLAB. The maximum output of the system was 80 db SPL.

Sp5 Stimulation

Sp5 neurons were activated by passing current through a bipolar concentric stimulating electrode (Frederick Haer and Co.) directed towards the left Sp5 using stereotaxic coordinates (0.28 cm left of midline, 0.2–0.3 cm caudal to the transverse sinus, 0.9 cm below surface of cerebellum). Current (4 pulses, 3/sec) amplitudes ranged from 10 to 90 μA.

In 5/7 experiments, the tip of the stimulating electrode was dipped in fluorogold before insertion to enable post mortem reconstruction of the electrode placements (see below). To assist in determining the correct locations while performing the experiment, a receptive field was recorded using the stimulating electrode as the active recording electrode. Regions of the face and head were stimulated using a custom-built mechanical stimulator that was driven by the TDT system.

Bimodal Stimulation

Bimodal stimuli consisted of a short burst of electrical stimulation in the Sp5 followed 10 ms later by a short BF tone burst (50 ms, 20 dB SL). For assessment of bimodal integration, responses to bimodal stimuli were compared to responses to acoustic stimuli (50 ms, BF tonebursts at 20 dB SL). Unimodal acoustic and bimodal trials were either performed as test-retest blocks (300 acoustic – 300 bimodal – 300 acoustic) or were randomly interleaved.

Data Acquisition

Recordings were made in a sound-attenuating single-walled booth. A four-shank, 16-channel silicon substrate electrode (100 microns between sites, 250 microns between shanks, 177 micron^2 site area, Neuronexus, Inc, Michigan) (Figure 2A,B) was used to record activity from many units simultaneously. Figure 2 shows the location of recording sites on the electrode array (Figure 2A) and their relative positions in the DCN (Figure 2B). We were able to sample from 16 locations within a small BF range without moving the probe. The electrode was inclined to an angle of 35–45° from vertical and positioned on the DCN surface 0.5–0.75 mm medial to the paraflocular recess. The tip of the electrode array was advanced 600 μm below the surface of the DCN in a ventro-rostral direction. If necessary, the electrode was repositioned until robust responses to ipsilateral acoustic stimulation were obtained.

The 16-channel electrode was connected by a 16-channel pre-amplifier and digitizer to a Tucker-Davis Technologies (TDT) data-acquisition system. The signals were filtered from 300–7500 Hz prior to analog-to-digital conversion. Analog-to-digital conversion was performed by simultaneous-sampling 12-bit converters at 25 kHz per channel. A spike detection threshold was set independently for each recording channel to four standard deviations (SDs) above the mean background noise voltage. Timestamps and associated waveforms were recorded at each threshold crossing.

Offline sorting

Spike waveforms exceeding 4 SDs above the RMS noise floor were detected at approximately 80% of the recording sites. The unit waveforms on each channel were sorted

using the Plexon Offline Sorter program (Plexon, Inc., Dallas, TX) with an automated cluster analysis of principal component amplitudes (Figure 2E). Units with more than 2% of spikes within a refractory window of 1 ms were excluded. Following sorting, unit waveforms were manually verified in terms of their amplitude consistency across trials and inter-spike intervals. In some cases, it was possible to sort waveforms from a single recording site into more than one unit that met statistical criteria ($p<0.05$) for independence, thus increasing our yield of individually isolated units.

Data analysis

On-line and post-experiment data analysis was performed in MATLAB. Peri-stimulus time histograms (PSTHs), response maps, rate-level functions, and thresholds were generated. A response threshold was taken to be the linearly interpolated sound level at which the difference in the mean spike rate between the driven response and the spontaneous activity satisfied a Student's t-test for statistical significance at a level of $p < 0.01$. This algorithm gave thresholds that agreed closely with visual inspection of PSTHs and rate-level functions. Threshold was also verified visually by comparing the response to the next higher level at which a strong response around the same latency was observed. Latency of the response to Sp5 stimulation was the point in time at which the firing rate was suppressed below the average firing rate or exceeded 2 SDs above the average firing rate preceding stimulation. Mean first spike latencies and first inter-spike intervals were computed for responses to BF tones (with or without Sp5 stimulation). The latency of the first spike and the interval between the first and second spikes after the onset of the tone stimulus were averaged across all trials for each stimulus condition. To assess regularity of firing to BF tones, inter-spike interval histograms and coefficients of variation (CVs) were calculated (Young, Robert et al. 1988; Parham and Kim 1992) using Neuroexplorer software (Nex Technologies, Littleton, MA). Both the transient CV (tCV, 0–10 ms post-acoustic onset) and the steady state CV (sCV, 15–45 ms post-acoustic onset) were computed. The effect of Sp5 stimulation on the firing rate of the response to BF tones was assessed using the degree of integration measure used in preceding work (Shore 2005) to allow for comparison. Bimodal enhancement (BE) was calculated as follows: $BE= [Bi-T-A)/(T+A)] \times 100$ where Bi is the number of spikes occurring during the bimodal response, T is the number of spikes occurring during the trigeminal response, and A is the number of spikes occurring during the acoustic response. Bimodal suppression was calculated as follows: $BS = [(Bi- Uni_{max})/Uni_{max}] \times 100$ where Uni_{max} is the maximum of T and A.

Response type classification

Units were classified based on the PSTH shape of their response to BF tones at 20 dB SL. As shown previously in the guinea pig (Stabler, Palmer et al. 1996), pyramidal cell responses typically fall into one of three temporal firing patterns: chopper units with highly regular, short latency spikes in response to BF tones can be classified as sustained or transient based on the duration of chopping (Hewitt and Meddis 1993). For the purposes of this study, transient and sustained choppers were combined into one class of chopper units. Buildup units fired irregular spikes with a longer latency. Pauser units were similar to buildup units, but had an additional short latency response.

Histology

The locations of the recording electrodes in the DCN and the stimulating electrode in the SP5 were verified post mortem. To mark the electrode tracks, the recording and stimulating electrodes were dipped in fluorogold (2%) before being inserted into the brain. At the end of each experiment, the animal was perfused transcardially with saline followed by 4% paraformaldehyde. The brain was removed from the skull and immersed in 20% sucrose solution (Zhou and Shore 2006). The following day, the brain was cryosectioned at 40–60

μm, placed on slides and examined under epifluorescence to document recording and stimulating locations.

Results

Recordings were obtained from 115 isolated single units with sufficient data for response-type classification (see Methods) in the pyramidal cell layer (layer II, 200–500μm from DCN surface) in response to BF tones preceded by Sp5 stimulation and to BF tones alone. The locations of the stimulating electrodes in Sp5 are shown in Figure 2C along with a multiunit receptive field recording obtained from the stimulating electrode while mechanically stimulating regions of the face and head (Figure 2D). The largest responses were obtained when the somatic surfaces of the face (skin and muscle) were stimulated. Movement of the jaw and tongue also elicited sizable responses.

Regularity of firing as measured by CV for responses to BF tones

Of the total number of classified units, 35 were chopper units (Figure 3A, D), 18 were buildup units (Figure 3B, D), and 33 were pauser units (Figure 3C, D). Twenty-nine units falling in between these categories are termed ‘unusual’ (Figure 3D). Of these 115 units, it was possible to compute the transient and steady state CV for a subset of units that responded to BF tones preceded by Sp5 stimulation and BF tones alone. The mean transient CV for BF tones was 0.77 +/− 0.11 (n=50), while the mean steady state CV was 0.65 +/− 0.07 (n=48). The distribution of transient CVs (Figure 3E) is broader than the distribution of steady state CVs (Figure 3F), although steady-state CVs tend to be lower (indicating more regularity). In the population of units recorded in this study, CVs were similarly distributed between 0.6 and 0.95 for all groups classified by PSTH of the BF response.

Unimodal responses to Sp5 stimulation are primarily excitatory

Unimodal responses to Sp5 stimulation were recorded from 94 of the 115 single units. The majority (52.1%) of measured responses were purely excitatory, while in 9.6% of the responses, the initial excitation was followed by inhibition. A few (7.4%) cells exhibited only inhibition. Approximately one-third (30.9%) of units did not exhibit a change in firing rate to Sp5 stimulation alone. However, 18/25 of these unimodally unresponsive units did show bimodal integration (see below), and are thus considered to have occult Sp5 inputs. The mean Sp5 stimulation thresholds (45μA +/− 16 s.d., n=53) were not significantly different between response types. However, the latencies of inhibitory responses (17.3 ms +/− 6.1 s.d., n=7) to Sp5 stimulation were significantly longer than for excitatory responses (11.5 ms +/− 4.2 s.d., n=47, unpaired t-test, $t(52) = -3.217$, $p=.002$) but no different than for complex responses (13.7 ms +/−5.2 s.d., n=9; unpaired t-test, $t(54) = -1.376$, $p=0.175$). Response durations were longer for complex responses (34.3 ms +/− 17.8 s.d., n=9) than for excitatory (25.4 ms +/− 17.8 s.d., n=47) or inhibitory (24.1 ms +/− 10.1 s.d., n=9) responses, but did not reach significance.

Prior Sp5 stimulation modulates sound-evoked firing patterns of pyramidal cells

Sp5 stimulation can decrease regularity in response to BF tones

In units classified as chopper, pauser or buildup (and thus likely to be pyramidal cells), the temporal firing patterns in response to BF tones were altered when the tone was preceded by Sp5 stimulation. The chopper unit shown in Figure 4A responded consistently to BF tones for six hundred trials over several minutes (Figure 4A1–A2), firing in a regular manner with an average spike rate of 260 spikes/sec. When Sp5 stimulation preceded the tone by 10 ms (Figure 4A3), the chopping pattern at the onset of the response was abolished and the

average spike rate decreased to 120 spikes/sec. When unimodal BF tone stimulation was retested without Sp5 stimulation, the neuron resumed its original firing pattern, and the firing rate partially recovered to 201 spikes per second (Figure 4A4–A5). The raster plots reveal that the firing in response to BF tones was regular (Figure 4B, Top, transient CV = 0.67, measured during the first 10 ms of the response) and became less regular (Figure 4B, Bottom, tCV = 0.88) when Sp5 was stimulated, consistent with the disappearance of chopping from the PSTH. The rate suppression induced by Sp5 stimulation was similar to the reduction in noise-evoked firing rate induced by trigeminal ganglion stimulation (Shore 2005; Shore, Koehler et al. 2008). Figure 4C shows the effect of Sp5 stimulation on a pauser unit. In this case, prior Sp5 stimulation decreased the average firing rate from 75 spikes/sec to 56 spikes/sec and induced a more consistent interval between the first and second spike, which is reflected in the decrease in tCV. Figure 4D shows another chopper unit in which there was a decrease in regularity with little change in the steady state firing rate of the neuron but an increase in the onset firing rate. Regularity changes can thus occur independently of rate changes after Sp5 stimulation (see Figure 6C for more detail on the relationship between regularity and firing rate). The changes in regularity appear to increase as the bimodal pairing continues from the first trial (bottom row of the raster) to the last trial (top row of the raster) in Figures 4C and 4D.

Changes in regularity by prior Sp5 stimulation depend on unimodal response regularity

Across the population of units with measurable CVs, the distribution after Sp5 stimulation of transient (Figure 5A) and steady-state (Figure 5C) CVs is broader and has a higher mean than the distribution of transient and steady-state CVs of acoustic responses (Figures 3D and 3F). Mean steady state CVs increased significantly from 0.64 +/− 0.06 s.d. to 0.67 +/− 0.09 s.d. with Sp5 stimulation (paired t-test, $t(45)= -2.090$, $p=0.042$) while mean transient CVs increased from 0.77 +/− 0.11 s.d. to 0.81 +/− 0.13 s.d. (paired t-test, $t(47)= -1.794$, $p=0.079$). Out of 46 units, 19 showed decreased transient CVs (increased regularity) and 27 showed increased transient CVs (decreased regularity) following Sp5 stimulation. Units that showed increased regularity had an average decrease in the transient CV of 16.3% while those that showed a decrease in regularity had an average increase in the transient CV of 13.8 %. Of the units with a change in regularity, 13/46 did not respond to unimodal Sp5 stimulation, indicating that timing changes can be independent of supra-threshold somatosensory responses.

The change in transient regularity with Sp5 stimulation was dependent on the initial regularity prior to Sp5 stimulation (Figure 5B, $r^2=0.28$, $F(1,46) = 17.869$, $p<0.001$). When the transient acoustic response was more regular (left side of graph), the response tended to be less regular with Sp5 stimulation, i.e. its CV increased (points above the horizontal line). When the acoustic response was less regular (right side of graph) the acoustic response became more regular (i.e., its transient CV decreased) with Sp5 stimulation. Although this observation is clearest for the transient regularity measurements (Figure 5B), it is also apparent for the steady-state portion of the response (sCV, Figure 5D, $R^2=0.156$, $F(1,44) = 8.130$, $p=.007$).

Prior Sp5 stimulation enhances or suppresses firing rate of the acoustically evoked response

Bimodal integration was quantified in 69 units using the “degree of integration” index (see Methods), which measures how much the firing rate of the bimodal response surpasses the linear summation of the responses to sound and Sp5 stimulation alone. Thirty eight percent of units showed bimodal enhancement while 40.6% of units showed bimodal suppression. The remaining 21.7% did not show bimodal integration. There was a mean increase in firing

rate of 35.3% in units showing enhancement, while there was a mean reduction in firing rate of 24.3% in units showing suppression. Interestingly, unit type was an important factor in whether bimodal integration was enhancing or suppressive, as described below.

Chopper units show bimodal enhancement and buildup units show bimodal suppression

Figure 6A shows that chopper unit responses were typically enhanced, while buildup unit responses were mostly suppressed by Sp5 stimulation. Pauser and unusual units showed both suppressive and enhancing bimodal integration.

The temporal changes in bimodal responses do not depend on the change in firing rate

The increase in regularity was not significantly correlated with the degree of bimodal integration (R^2=.014, F(1,28) = 0.387, p = 0.539; Figure 6B). However, suppression of the firing rate by bimodal stimulation (left half of figure 6B) was more often (7 vs. 3 units) accompanied by an increase in regularity of the response (i.e., a decrease in the CV). Enhancement of the firing rate (right half of Figure 6B) was more often (10 vs. 7 units) accompanied by a decrease in the regularity of the response (i.e., an increase in the CV).

Additionally, the change in CV in units that did show rate integration is similar to the change in CV in units that did **not** show rate integration (data not shown). As the CV measure itself is not independent of spike rate, we examined the relationship between change in CV and change in spike rate in figure 6C. The transient CV shows a weak but significant correlation (r^2=0.111, F(1,45) = 5.596, p = 0.022) with firing rate measured in the same time window indicating that the variation in firing rate explains 10 % of the variation in tCV. However, the effect that is shown in Figure 6C is the opposite of what would be expected from rate-dependent effects for which, at higher rates, the effects of the refractory period should lead to lower CV values (i.e., more “regularity” because the spike interval distribution is compressed by the effects of the refractory period). In addition, at lower rates, the effect of the refractory period would become less (as a function of rate), and so the correlation should decrease, and the CV should become (relatively) larger instead of smaller, as observed. Thus, factors other than firing rate contribute to the changes in regularity.

Prior Sp5 stimulation increases the acoustic response latency

The mean first spike latency (FSL) of the response to BF tones was calculated for 74 single units responding to BF tones alone and to BF tones preceded by Sp5 stimulation. Figure 7A shows one example of a FSL shift, in which Sp5 stimulation increased the FSL averaged over 200 trials from 25.5 ms to 27.8 ms. Sp5 stimulation shortened the FSL in 24.3% of units by an average of 3.64 ms and lengthened the FSL in 75.7% of units by an average of 5.62 ms. Sixty nine percent of the units had a shorter FISI (average decrease of 4.31 ms +/− 2.83 s.d.) and 32% of the units had a longer FISI (average increase of 1.84 ms +/− 1.58 s.d.). The changes in FISI and FSL were positively correlated (Figure 7B; r^2=0.212, F(1,70) = 18.885, p < 0.001).

Mean FSL increased in units that were suppressed by Sp5 stimulation but did not respond to unimodal Sp5 stimulation

Even units that did not overtly respond to unimodal Sp5 stimulation had significantly longer latencies to sound when preceded by Sp5 stimulation (NR, Figure 7C; ANOVA adjusted for unequal variances with post-hoc Tukey’s test, d.f.=5, F=60.949, p<0.01). When the responses to BF tones were suppressed by Sp5 stimulation, the latency of the response also increased significantly (Figure 7D; ANOVA with post-hoc Tukey’s test, p<0.05).

Tonotopic organization of Sp5 influence on acoustic responses

The precise organization of the somatosensory inputs to the granule cell domains and their targets via the parallel fibers to DCN cells is not known. Our results suggest that the effects of Sp5 stimulation on firing rate and latency of acoustic responses vary along the tonotopic axis of the nucleus. Bimodal rate suppression progressively increases from low to high and is largest in the 10 kHz best frequency region (Figure 8A, Left). On the other hand, the strength of bimodal rate enhancement shows no apparent trend across best frequencies (Figure 8A, Right). The FSL also shows a best-frequency-dependent increase, being largest between 7 and 10 kHz, with no change on average below 5 kHz or above 12 kHz (Figure 8B, Left). In units with a decrease in the response latency, there is no dependence of the decrease on the BF of the unit (Figure 8B, Right). Changes in the transient CV with bimodal stimulation are slightly larger at middle frequencies (7–10 kHz) (Figure 8C, Left and Right). These results suggest that bimodal integration systematically affects processing in middle frequencies (~10 kHz) of the guinea pig hearing range.

Discussion

These experiments show that multisensory integration at the first stages of auditory processing can affect not only average spike rate, but also spike timing and the temporal representation of sounds in DCN principal neurons. First spike latency to tones and the regularity of subsequent firing is altered when Sp5 stimulation precedes sound. These changes can occur even in the absence of overt rate changes, suggesting that auditory-somatosensory integration is represented in the DCN in the timing of spikes, as is seen in visual-auditory integration in sub-cortical regions (Zahar, Reches et al. 2009).

The latency of firing of DCN pyramidal cells can be shifted by prior hyperpolarization as shown by *in vitro* experiments (Manis 1990; Kanold and Manis 1999; Kanold and Manis 2001; Kanold and Manis 2005). The latency shifts can occur for membrane potential changes that precede a depolarization by as much as 100 ms, and depend on rapidly inactivating transient potassium currents that are de-inactivated by the hyperpolarization (Kanold and Manis 1999; Kanold and Manis 2001; Kanold and Manis 2005). In the present experiments, even though the inhibitory effects on spontaneous activity by Sp5 stimulation had mostly faded prior to the acoustic stimulation, the ensuing latency shift would be consistent with transient potassium current involvement, which can hold the memory of prior hyperpolarization (Kanold and Manis 2001; Kanold and Manis 2005). On the other hand, in some units, prior Sp5 stimulation increased the response latency with no observable effect of Sp5 stimulation alone. It is unclear whether this is due to weak hyperpolarization, or the presence of a separate source of inhibition from Sp5 that is gated by acoustic stimulation. However, the increased latency of sound-evoked responses after Sp5-induced suppression of spontaneous activity could also be explained by a long-lasting inhibition. One putative source of the inhibition could be cartwheel cells that can hyperpolarize pyramidal cells to −68 mV (Golding and Oertel 1997) which in turn can generate a latency increase between 2 and > 25 ms *in vitro* (Kanold and Manis, 2001).

The latency changes described here may be decoded by time sensitive neurons at the next stage of processing in the inferior colliculus (see Kanold and Manis, 2005), as has been also been postulated for latency changes in T-stellate neurons that are inhibited by D-stellate neurons in the ventral cochlear nucleus (Needham and Paolini 2006). The DCN may be involved in suppression of self-generated vocalizations or more generally by sounds associated with self-generated movement (Bell, Bodznick et al. 1997). Activation of somatosensory inputs by self-generated movement may “tune” pyramidal cells to transmit a reduced response to coincident sounds by increasing the first spike latency. This increased latency could correspond to a reduction in gain in the spike latency code for intensity, since

intensity and latency are often inversely related (Heil 2004). The DCN is also thought to play a role in sound localization through its sensitivity to spectral notches in the head-related transfer function (Young, Spirou et al. 1992; Imig, Bibikov et al. 2000; Reiss and Young 2005). Sound localization cues, including spectral notches, are better represented by first spike times than by average firing rate in neurons in the inferior colliculus targets of the pyramidal cells (Chase and Young 2006). By shifting the first spike latency, somatosensory input to the CN could emphasize or de-emphasize particular responses to spectral notches or other acoustic features depending on the position of the head (in guinea pigs) or the position of the pinnae (in cats).

Another measure of temporal information is spike regularity, as measured here by the CV (Young, Robert et al. 1988; Parham and Kim 1992). Higher CV measurements in this preparation as compared to cat (Parham and Kim 1992) and guinea pig (Stabler, Palmer et al. 1996) preparations may be due to differences in anesthetic (ketamine-xylazine versus pentobarbital), recording electrodes (silicon substrate multi-channel electrodes), or stimulus intensity (60 dB SPL). Ketamine is an antagonist to NMDA receptors and may reduce glutamatergic neurotransmission from parallel fibers to cartwheel and pyramidal cells (Sinner and Graf 2008). There are also indications that ketamine may reduce glycinergic inhibition, which could weaken the inhibition of pyramidal cells by cartwheel cells (Wang, Huang et al. 2005). Thus, the effect of anesthesia might diminish both the effects of glutamatergic somatosensory inputs on granule cells as well as glycinergic inhibition of cartwheel cells on pyramidal cell firing. The results presented here thus likely under represent the putative effects of the somatosensory influence on spike timing, which would be predicted to be stronger in awake animals. Future studies will address these issues in awake animals with more natural, direct somatosensory stimulation.

Our results show that Sp5 stimulation can either increase or decrease the regularity of sound-evoked spikes, depending on the unit's regularity in the absence of Sp5 stimulation. If a common set of mechanisms is responsible for the regularity changes as well as the firing rate and latency changes, we might expect the shifts in these measures following Sp5 stimulation to be correlated across the population of units. As discussed above, latency changes following Sp5 stimulation were correlated with changes in firing rate. However, the effects of Sp5 stimulation on regularity and rate integration were independent, suggesting that multiple mechanisms are engaged by Sp5 pathways. Discharge regularity is influenced by relative contributions of synaptic versus intrinsic ionic mechanisms, or even different intrinsic mechanisms, and can vary with the rate of synaptic inputs and the discharge rate (Street and Manis 2007).

In the present study, changes in regularity occurred even in units in which there was no measurable response to unimodal Sp5 stimulation. This could be explained by findings that perturbation of the membrane potential (even subthreshold perturbations) prior to acoustic stimulation can engage multiple, long-lasting effects on discharge patterns. For example, in quiescent DCN pyramidal cells, prior activity can affect spike latency and subthreshold oscillations for as long as 800 msec (Manis, Molitor et al. 2003). In pyramidal cells driven by dynamic stimuli, brief hyperpolarizations affect spike timing for up to 300 ms, while brief depolarizations have weaker and shorter-lasting effects (Street and Manis 2007). Although the mechanisms for the *in vitro* phenomena have not been fully elucidated, they meet the requirements to underlie the changes in discharge regularity shown here. They are specifically engaged by prior shifts in membrane potential, and their effects persist long after the membrane potential has decayed to the resting level prior to stimulation. This relationship will need to be substantiated using intracellular recordings in the *in vivo* model.

Another set of mechanisms that could modulate the discharge patterns is the activation of metabotropic receptor systems in the DCN, such as $GABA_B$ receptors that are localized to parallel fibers and apical pyramidal cell dendrites (Evans and Zhao 1993; Juiz, Albin et al. 1994; Lujan, Shigemoto et al. 2004) and mGluR receptors, which are localized to cartwheel cell dendrites (Wright, Blackstone et al. 1996; Molitor and Manis 1997; Mugnaini, Dino et al. 1997; Rubio and Wenthold 1997; Petralia, Rubio et al. 2000; Spatz 2001). These mechanisms could be driven within the DCN by Sp5 synaptic activity, and could regulate the strength (Fujino and Oertel 2003) or dynamics of subsequent synaptic transmission within the DCN circuit. They can also be coupled to the regulation of ion channel availability or channel kinetics in postsynaptic cells.

The bi-directional effect of Sp5 stimulation on firing rate (41% suppression; 38 % enhancement), latency (75% of units had longer latencies, 25% of units had shorter latencies), and regularity (57% of units had decreased regularity; 43% of units had increased regularity) implies that there is variability in the underlying mechanisms, with a bias towards inhibition. For example, the same Sp5 stimulus resulting in increases and decreases in latency in different units could be due to the heterogeneous distribution of potassium channel subtypes in pyramidal cells (Rusznak, Bakondi et al. 2008). Alternatively, projections from different regions of Sp5 may activate different patterns of excitatory and inhibitory synaptic activity in pyramidal cells and could be responsible for the heterogeneous effects. The tonotopic organization of Sp5 effects shown here supports the idea that the Sp5 stimulation site and the pattern of innervation in the DCN from that stimulation site could contribute to the observed variability in rate and timing effects.

DCN pyramidal cells integrate Sp5 and acoustic inputs with features both in common with and distinct from those shown previously for trigeminal ganglion stimulation (Shore 2005; Shore, Koehler et al. 2008). A common feature is the presence of bimodal enhancement or suppression of firing rate in 80% of neurons recorded. However, several differences are also apparent. While trigeminal ganglion stimulation primarily suppressed sound-evoked firing rates, Sp5 stimulation only showed slightly more suppression of acoustic response rates. Furthermore, while unimodal trigeminal ganglion stimulation resulted in approximately equal numbers of excited or inhibited units, unimodal Sp5 responses were primarily excitatory (Shore, 2005; Shore et al., 2008). Despite the predominance of excitation following unimodal Sp5 stimulation, the increased latencies and suppression of acoustic responses by Sp5 stimulation suggests a predominant inhibitory effect of Sp5 on sound-driven responses. Indeed, the known anatomical connections and physiological effects (Young, Nelken et al. 1995; Davis and Young 1997; Kanold and Young 2001) make it likely that additional sub-threshold inhibitory circuits are activated by Sp5 stimulation.

The responses of pyramidal cells to Sp5 stimulation may also depend on the organization of the projections from Sp5 onto the tonotopic axes of the DCN. Sp5 stimulation produced a larger suppression of firing rate and increases in latency within the mid-frequency region (~10 kHz) of the DCN. The peripheral representation of inputs to the DCN via Sp5 appears to be principally from the face areas (see Figure 2), but not from the pinnae region, which is principally carried via the cuneate nucleus pathways (Kanold and Young 2001). This suggests that the Sp5 pathways are more likely involved with suppression of self-generated sound (Haenggeli, Pongstaporn et al. 2005;Shore 2005) than with sound localization in the vertical plane that depends on pinnae cues (Masterton, Granger et al. 1994;Huang and May 1996). However, guinea pig vocalizations cover a wide frequency range (Wallace and Palmer 2008), so it is not clear why the Sp5 inputs should show a frequency-specific modulation of DCN activity.

Significance of Findings

The modulation of DCN spike timing by somatosensory inputs as demonstrated here suggests that this circuitry could significantly alter the representation of the acoustic environment by pyramidal cells. For example, changing the temporal response pattern from a chopper to a buildup pattern could result in a code that reports aspects of stimulus duration, whereas changing from a buildup to a pauser pattern might result in a code that signifies the stimulus onset. Similarly, changes in regularity could lead to increased (or decreased) synchronous firing of populations of pyramidal cells, and thus alter their synaptic influence onto inferior colliculus neurons.

Under conditions of sensory deprivation induced by cochlear damage, somatosensory influences on the CN are enhanced (Shore, Koehler et al. 2008; Zeng, Nannapaneni et al. 2009). Similar cochlear insults give rise to phantom perceptions of sound, or tinnitus (Kaltenbach, Zhang et al. 2005). Thus, we might expect that the spike- timing alterations observed here would be further enhanced under conditions that cause tinnitus. These spike-timing alterations may explain the ability of patients to modulate the pitch and loudness of their tinnitus by manipulations of their face and neck (Levine 1999; Levine, Abel et al. 2003; Biesinger, Reisshauer et al. 2008), regions that are innervated by the trigeminal nerve.

Acknowledgments

This work was supported by NIH P01 DC00078, R01 DC004825 (SES), T32 DC000011 (SDK), R01 DC000425 (PBM) and the Tinnitus Research Consortium. We would like to thank Chris Ellinger, Dwayne Vailliencourt and Ben Yates for expert technical assistance.

Abbreviations

BF	Best Frequency
CN	Cochlear Nucleus
CV	Coefficient of Variation
DCN	Dorsal Cochlear Nucleus
FSL	Mean First Spike Latency
FISI	Mean First Inter-Spike Interval
Sp5	Spinal Trigeminal Nucleus

References

Bell C, Bodznick D, et al. The generation and subtraction of sensory expectations within cerebellum-like structures. Brain Behav Evol. 1997; 50(Suppl 1):17–31. [PubMed: 9217991]

Biesinger E, Reisshauer A, et al. The role of the cervical spine and the craniomandibular system in the pathogenesis of tinnitus. Somatosensory tinnitus. HNO. 2008; 56(7):673–677. [PubMed: 18560742]

Chase SM, Young ED. Spike-timing codes enhance the representation of multiple simultaneous sound-localization cues in the inferior colliculus. J Neurosci. 2006; 26(15):3889–3898. [PubMed: 16611804]

Davis KA, Miller RL, et al. Effects of somatosensory and parallel-fiber stimulation on neurons in dorsal cochlear nucleus. J Neurophysiol. 1996; 76(5):3012–3024. [PubMed: 8930251]

Davis KA, Young ED. Granule cell activation of complex-spiking neurons in dorsal cochlear nucleus. J Neurosci. 1997; 17(17):6798–6806. [PubMed: 9254690]

Evans EF, Zhao W. Varieties of inhibition in the processing and control of processing in the mammalian cochlear nucleus. Prog Brain Res. 1993; 97:117–126. [PubMed: 7901869]

Fujino K, Oertel D. Bidirectional synaptic plasticity in the cerebellum-like mammalian dorsal cochlear nucleus. Proc Natl Acad Sci U S A. 2003; 100(1):265–270. [PubMed: 12486245]

Golding NL, Oertel D. Physiological identification of the targets of cartwheel cells in the dorsal cochlear nucleus. J Neurophysiol. 1997; 78(1):248–260. [PubMed: 9242277]

Haenggeli CA, Pongstaporn T, et al. Projections from the spinal trigeminal nucleus to the cochlear nucleus in the rat. J Comp Neurol. 2005; 484(2):191–205. [PubMed: 15736230]

Heil P. First-spike latency of auditory neurons revisited. Curr Opin Neurobiol. 2004; 14(4):461–467. [PubMed: 15321067]

Hewitt MJ, Meddis R. Regularity of cochlear nucleus stellate cells: a computational modeling study. J Acoust Soc Am. 1993; 93(6):3390–3399. [PubMed: 8326065]

Huang AY, May BJ. Sound orientation behavior in cats. II. Mid-frequency spectral cues for sound localization. J Acoust Soc Am. 1996; 100(2 Pt 1):1070–1080. [PubMed: 8759960]

Imig TJ, Bibikov NG, et al. Directionality derived from pinna-cue spectral notches in cat dorsal cochlear nucleus. J Neurophysiol. 2000; 83(2):907–925. [PubMed: 10669504]

Juiz JM, Albin RL, et al. Distribution of GABAA and GABAB binding sites in the cochlear nucleus of the guinea pig. Brain Res. 1994; 639(2):193–201. [PubMed: 8205472]

Kaltenbach JA, Zhang J, et al. Tinnitus as a plastic phenomenon and its possible neural underpinnings in the dorsal cochlear nucleus. Hear Res. 2005; 206(1–2):200–226. [PubMed: 16081009]

Kanold PO, Manis PB. Transient potassium currents regulate the discharge patterns of dorsal cochlear nucleus pyramidal cells. J Neurosci. 1999; 19(6):2195–2208. [PubMed: 10066273]

Kanold PO, Manis PB. A physiologically based model of discharge pattern regulation by transient K+ currents in cochlear nucleus pyramidal cells. J Neurophysiol. 2001; 85(2):523–538. [PubMed: 11160490]

Kanold PO, Manis PB. Encoding the timing of inhibitory inputs. J Neurophysiol. 2005; 93(5):2887–2897. [PubMed: 15625095]

Kanold PO, Young ED. Proprioceptive information from the pinna provides somatosensory input to cat dorsal cochlear nucleus. J Neurosci. 2001; 21(19):7848–7858. [PubMed: 11567076]

Kirzinger A, Jurgens U. Vocalization-correlated single-unit activity in the brain stem of the squirrel monkey. Exp Brain Res. 1991; 84(3):545–560. [PubMed: 1864326]

Levine RA. Somatic (craniocervical) tinnitus and the dorsal cochlear nucleus hypothesis. Am J Otolaryngol. 1999; 20(6):351–362. [PubMed: 10609479]

Levine RA, Abel M, et al. CNS somatosensory-auditory interactions elicit or modulate tinnitus. Exp Brain Res. 2003; 153(4):643–648. [PubMed: 14600798]

Lujan R, Shigemoto R, et al. Localization of the GABAB receptor 1a/b subunit relative to glutamatergic synapses in the dorsal cochlear nucleus of the rat. J Comp Neurol. 2004; 475(1):36–46. [PubMed: 15176083]

Luthe L, Hausler U, et al. Neuronal activity in the medulla oblongata during vocalization. A single-unit recording study in the squirrel monkey. Behav Brain Res. 2000; 116(2):197–210. [PubMed: 11080551]

Manis PB. Membrane properties and discharge characteristics of guinea pig dorsal cochlear nucleus neurons studied in vitro. J Neurosci. 1990; 10(7):2338–2351. [PubMed: 2376777]

Manis PB, Brownell WE. Synaptic organization of eighth nerve afferents to cat dorsal cochlear nucleus. J Neurophysiol. 1983; 50(5):1156–1181. [PubMed: 6644365]

Manis PB, Molitor SC, et al. Subthreshold oscillations generated by TTX-sensitive sodium currents in dorsal cochlear nucleus pyramidal cells. Exp Brain Res. 2003; 153(4):443–451. [PubMed: 14508631]

Masterton RB, Granger EM, et al. Role of acoustic striae in hearing: mechanism for enhancement of sound detection in cats. Hear Res. 1994; 73(2):209–222. [PubMed: 8188550]

May BJ. Role of the dorsal cochlear nucleus in the sound localization behavior of cats. Hear Res. 2000; 148(1–2):74–87. [PubMed: 10978826]

Meredith MA, Keniston LR, et al. Crossmodal projections from somatosensory area SIV to the auditory field of the anterior ectosylvian sulcus (FAES) in Cat: further evidence for subthreshold forms of multisensory processing. Exp Brain Res. 2006; 172(4):472–484. [PubMed: 16501962]

Molitor SC, Manis PB. Evidence for functional metabotropic glutamate receptors in the dorsal cochlear nucleus. J Neurophysiol. 1997; 77(4):1889–1905. [PubMed: 9114243]

Mugnaini E, Dino MR, et al. The unipolar brush cells of the mammalian cerebellum and cochlear nucleus: cytology and microcircuitry. Prog Brain Res. 1997; 114:131–150. [PubMed: 9193142]

Needham K, Paolini AG. Neural timing, inhibition and the nature of stellate cell interaction in the ventral cochlear nucleus. Hear Res. 2006; 216–217:31–42.

Oertel D, Young ED. What's a cerebellar circuit doing in the auditory system? Trends Neurosci. 2004; 27(2):104–110. [PubMed: 15102490]

Parham K, Kim DO. Analysis of temporal discharge characteristics of dorsal cochlear nucleus neurons of unanesthetized decerebrate cats. J Neurophysiol. 1992; 67(5):1247–1263. [PubMed: 1597710]

Petralia RS, Rubio ME, et al. Differential distribution of glutamate receptors in the cochlear nuclei. Hear Res. 2000; 147(1–2):59–69. [PubMed: 10962173]

Populin L, Yin T. Bimodal interactions in the superior colliculus of the behaving cat. Journal of Neuroscience. 2002; 22(7):2826. [PubMed: 11923447]

Reiss LA, Young ED. Spectral edge sensitivity in neural circuits of the dorsal cochlear nucleus. J Neurosci. 2005; 25(14):3680–3691. [PubMed: 15814799]

Rubio ME, Wenthold RJ. Glutamate receptors are selectively targeted to postsynaptic sites in neurons. Neuron. 1997; 18(6):939–950. [PubMed: 9208861]

Rusznak Z, Bakondi G, et al. Voltage-gated potassium channel (Kv) subunits expressed in the rat cochlear nucleus. J Histochem Cytochem. 2008; 56(5):443–465. [PubMed: 18256021]

Saade NE, Frangieh AS, et al. Dorsal column input to cochlear neurons in decerebrate-decerebellate cats. Brain Res. 1989; 486(2):399–402. [PubMed: 2731042]

Shore SE. Multisensory integration in the dorsal cochlear nucleus: unit responses to acoustic and trigeminal ganglion stimulation. Eur J Neurosci. 2005; 21(12):3334–3348. [PubMed: 16026471]

Shore SE, Koehler S, et al. Dorsal cochlear nucleus responses to somatosensory stimulation are enhanced after noise-induced hearing loss. Eur J Neurosci. 2008; 27(1):155–168. [PubMed: 18184319]

Sinner B, Graf BM. Ketamine. Handb Exp Pharmacol. 2008; (182):313–333. [PubMed: 18175098]

Spatz WB. Unipolar brush cells in the human cochlear nuclei identified by their expression of a metabotropic glutamate receptor (mGluR2/3). Neurosci Lett. 2001; 316(3):161–164. [PubMed: 11744227]

Stabler SE, Palmer AR, et al. Temporal and mean rate discharge patterns of single units in the dorsal cochlear nucleus of the anesthetized guinea pig. J Neurophysiol. 1996; 76(3):1667–1688. [PubMed: 8890284]

Stein, B.; Meredith, M. The Merging of the Senses. Cambridge, MA: MIT Press; 1993.

Stein BE, Meredith MA. Multisensory integration. Neural and behavioral solutions for dealing with stimuli from different sensory modalities. Ann N Y Acad Sci. 1990; 608:51–65. discussion 65–70. [PubMed: 2075959]

Street SE, Manis PB. Action potential timing precision in dorsal cochlear nucleus pyramidal cells. J Neurophysiol. 2007

Wallace MN, Palmer AR. Laminar differences in the response properties of cells in the primary auditory cortex. Exp Brain Res. 2008; 184(2):179–191. [PubMed: 17828392]

Wang X, Huang ZG, et al. Ketamine inhibits inspiratory-evoked gamma-aminobutyric acid and glycine neurotransmission to cardiac vagal neurons in the nucleus ambiguus. Anesthesiology. 2005; 103(2):353–359. [PubMed: 16052118]

Wright DD, Blackstone CD, et al. Immunocytochemical localization of the mGluR1 alpha metabotropic glutamate receptor in the dorsal cochlear nucleus. J Comp Neurol. 1996; 364(4): 729–745. [PubMed: 8821458]

Wright DD, Ryugo DK. Mossy fiber projections from the cuneate nucleus to the cochlear nucleus in the rat. J Comp Neurol. 1996; 365(1):159–172. [PubMed: 8821448]

Young ED, Nelken I, et al. Somatosensory effects on neurons in dorsal cochlear nucleus. J Neurophysiol. 1995; 73(2):743–765. [PubMed: 7760132]

Young ED, Robert JM, et al. Regularity and latency of units in ventral cochlear nucleus: implications for unit classification and generation of response properties. J Neurophysiol. 1988; 60(1):1–29. [PubMed: 3404211]

Young ED, Spirou GA, et al. Neural organization and responses to complex stimuli in the dorsal cochlear nucleus. Philos Trans R Soc Lond B Biol Sci. 1992; 336(1278):407–413. [PubMed: 1354382]

Zahar Y, Reches A, et al. Multisensory enhancement in the optic tectum of the barn owl: spike count and spike timing. J Neurophysiol. 2009; 101(5):2380–2394. [PubMed: 19261710]

Zeng C, Nannapaneni N, et al. Cochlear damage changes the distribution of vesicular glutamate transporters associated with auditory and nonauditory inputs to the cochlear nucleus. J Neurosci. 2009; 29(13):4210–4217. [PubMed: 19339615]

Zhou J, Nannapaneni N, et al. Vessicular glutamate transporters 1 and 2 are differentially associated with auditory nerve and spinal trigeminal inputs to the cochlear nucleus. J Comp Neurol. 2007; 500(4):777–787. [PubMed: 17154258]

Zhou J, Shore S. Projections from the trigeminal nuclear complex to the cochlear nuclei: A retrograde and anterograde tracing study in the guinea pig. J Neurosci Res. 2004; 78(6):901–907. [PubMed: 15495211]

Zhou J, Shore S. Convergence of spinal trigeminal and cochlear nucleus projections in the inferior colliculus of the guinea pig. J Comp Neurol. 2006; 495(1):100–112. [PubMed: 16432905]

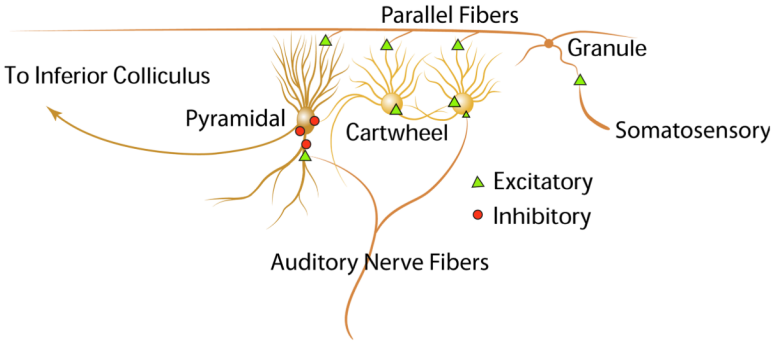

Figure 1.
Schematic illustrating known anatomical and physiological components of relevant DCN circuitry. Direct auditory input to pyramidal cells arrives via excitatory terminals on their basal dendrites. Spinal trigeminal nucleus (Sp5) input to pyramidal cells is indirect via granule cells. Granule cell axons, the parallel fibers, directly excite pyramidal cells through terminals on apical dendrites of pyramidal cells and inhibit pyramidal cells through inhibitory interneurons, the cartwheel cells

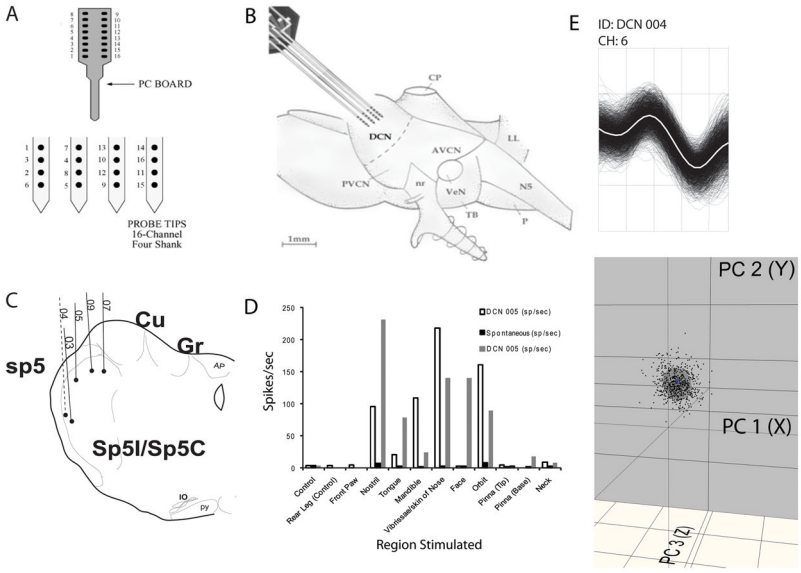

Figure 2.

A. Responses were recorded using a sixteen channel silicon substrate electrode array. Channels are arranged on four shanks in a 4×4 grid. B. The electrode array was visually placed into the DCN in a rostral-caudal/dorsal-ventral plane from the surface of the DCN. C. Schematic of histological reconstruction of the stimulating electrode tracks for 5/7 guinea pigs. D. A receptive field is constructed by plotting spike activity recorded from the Sp5 stimulating electrode in response to mechanical stimulation of various sites in the head and neck region. Black bars indicate spontaneous activity. White (05), see Figure 2C for Sp5 electrode position) and grey (06, see Figure 2C for Sp5 electrode position) bars indicate the level of spike activity in two different guinea pigs elicited by mechanical stimulation of the described region. E. Spike waveforms were sorted and single units identified. Detected spike waveforms were overlaid to aid in verification of consistent waveform shape and size (top). Thick gray line is an average of all spike waveforms. Principal component analysis was used in three dimensions to identify clusters of waveforms (bottom).

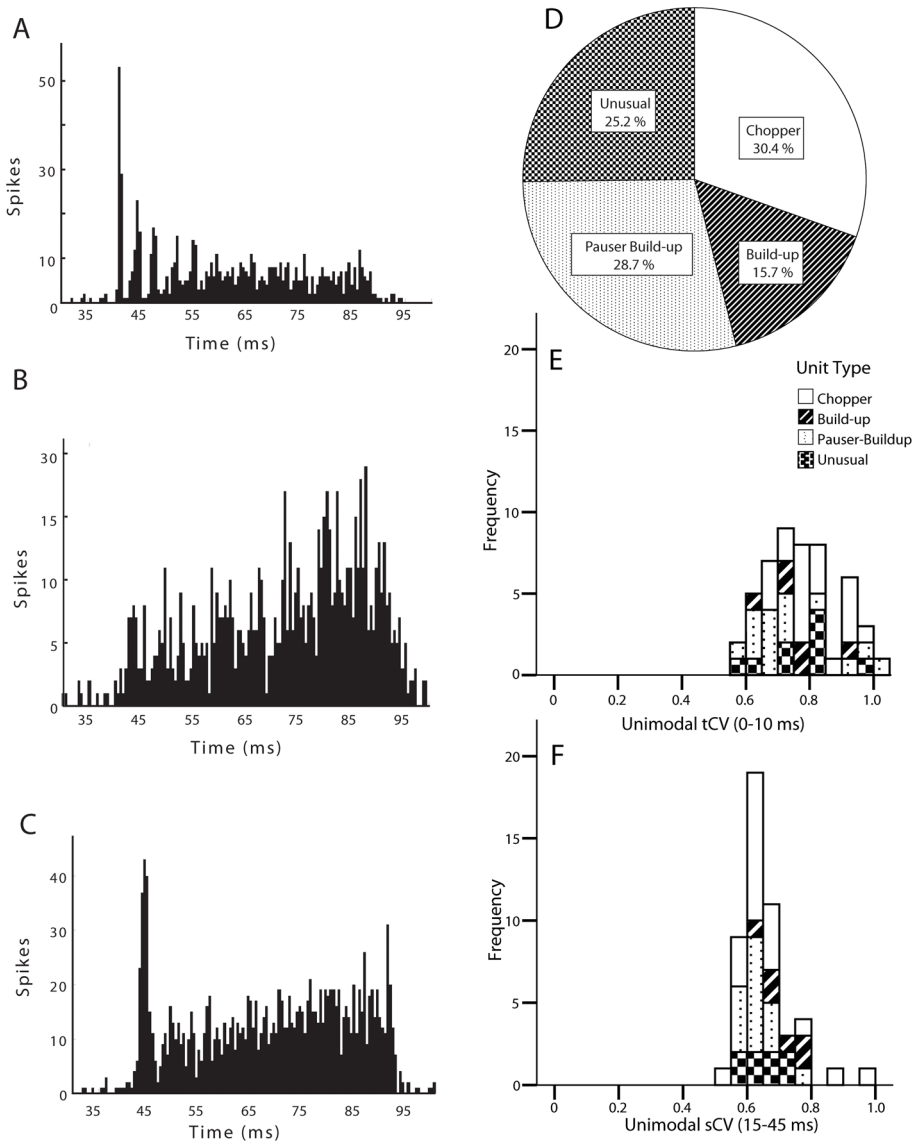

Figure 3.

PSTHs of DCN unit responses to BF tones at 20 dB SL. Bin width = 1 ms. 200 Trials. A. Chopper response type. B. Buildup response type. C. Pauser response type. D. Percentage of units that were classified as each type. Some unit responses were unusual. E. Histogram represents the distribution of transient CVs (0–10 ms post stimulus onset) measured from units responding to BF tones at 20 dB SL. F. Histogram represents the distribution of steady-state CVs (15–45 ms post stimulus onset) measured from units responding to BF tones at 20 dB SL.

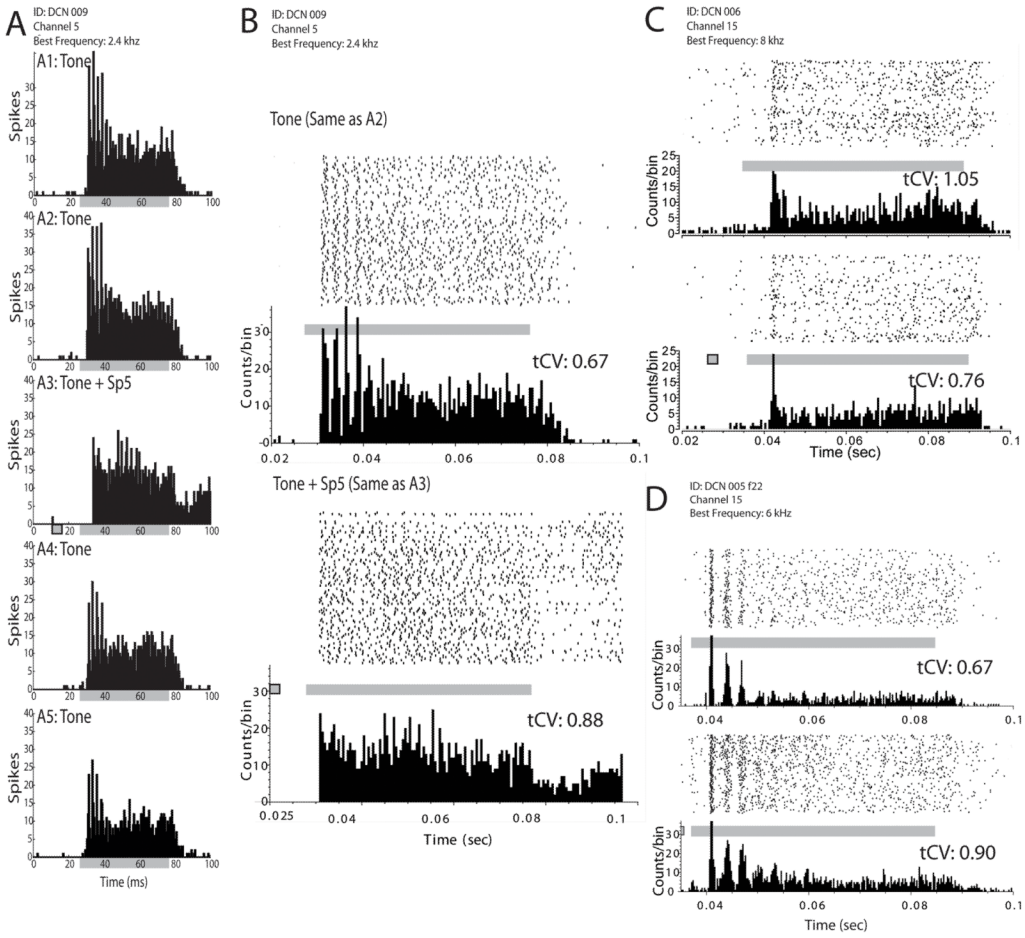

Figure 4.

Sp5 stimulation changes firing rate and regularity in DCN pyramidal cells. Firing rate is suppressed and regularity of the acoustic response is decreased when sound is preceded by Sp5 stimulation. A: A1 and A2. Identical responses of a chopper unit response to BF tones are shown prior to bimodal stimulation. A3. Bimodal response showing suppressive integration. A4–A5. Partially recovered acoustic responses at 5 and 10 minutes following the collection of bimodal responses. B. Raster plot and PSTH of a chopper unit response to BF tones (top, same as A2) and BF tones preceded by Sp5 stimulation (bottom, same as A3).C. Raster plot and PSTH of a pauser unit response to BF tones (top) and BF tones preceded by Sp5 stimulation (bottom). D. Raster plot and PSTH of a chopper unit response to BF tones (top) and BF tones preceded by Sp5 stimulation (bottom). Each PSTH is composed of 200 trials. In each raster plot, each point represents a spike and each row represents a single stimulus trial. The bottom row is the first trial. Solid gray bars indicate the duration of the acoustic stimulus. Gray bars with black borders indicate the duration of electrical stimulation of Sp5. The average value of the transient CV (tCV, see methods) is indicated above each response in B, C and D.

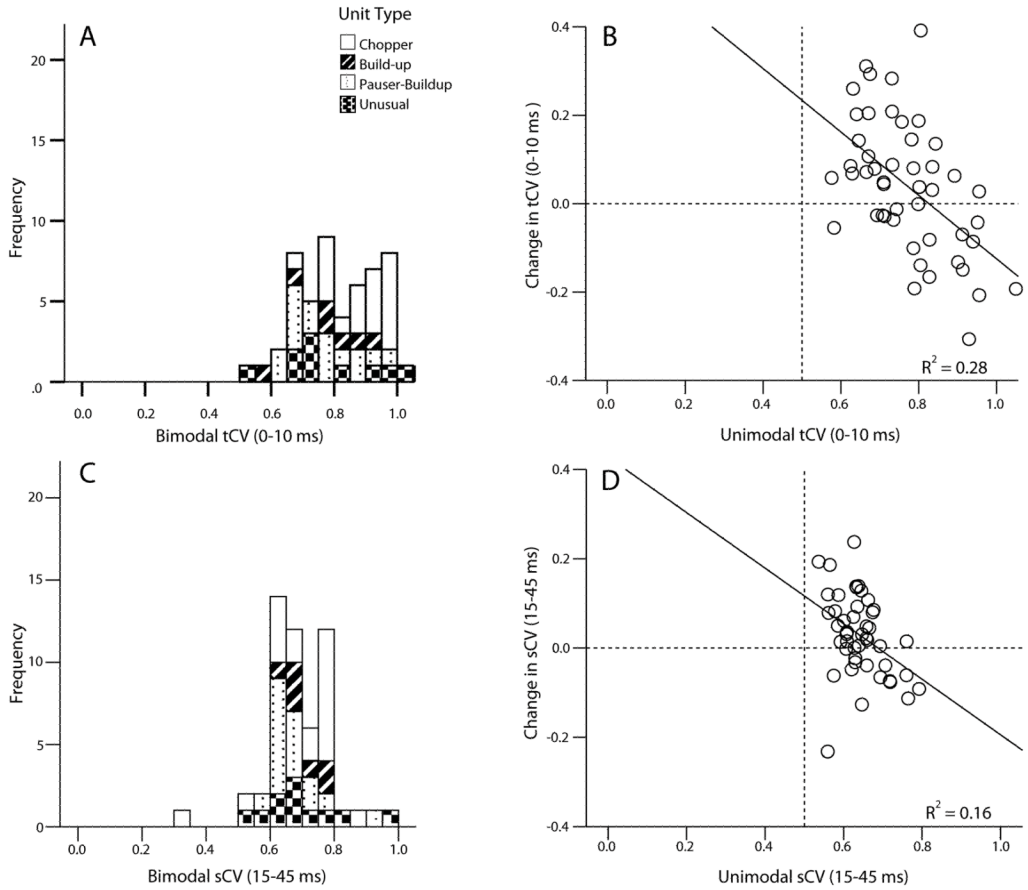

Figure 5.

Sp5-induced changes in regularity depend on the regularity of the acoustic response. A. The distribution of transient CVs (0–10 ms post stimulus onset) measured from units responding to bimodal stimulation (BF tones at 20 dB SL preceded by Sp5 stimulation). B. The change in transient CV with bimodal stimulation is plotted against the transient CV in response to sound. C. The distribution of steady-state CVs (15–45 ms post stimulus onset) measured from units responding to bimodal stimulation (BF tones at 20 dB SL preceded by Sp5 stimulation). D. Change in steady-state CV with bimodal stimulation is plotted against the steady-state CV in response to sound. C–D. Dashed vertical line separates regular units (Left, CV<0.5) from irregular units (Right, CV>0.5). Dashed horizontal line separates units that become less regular (Above Line) from units that become more regular (Below Line).

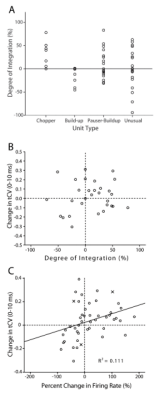

Figure 6.

Enhancement and suppression of acoustic responses by Sp5 stimulation. A. The degree of suppression or enhancement in chopper (C), buildup (B), pauser (PB), and unusual units. B. The change in CV is independent of the degree of integration. C. The change in tCV depends in part on the change in firing rate. Units from Figure 4B–D are identified with an x. B. and C. Units that become more regular are below the dashed horizontal line while units that become less regular are above it. Units that have increased firing rates are to the right of the dashed vertical line while units that have decreased firing rates are to the left of it.

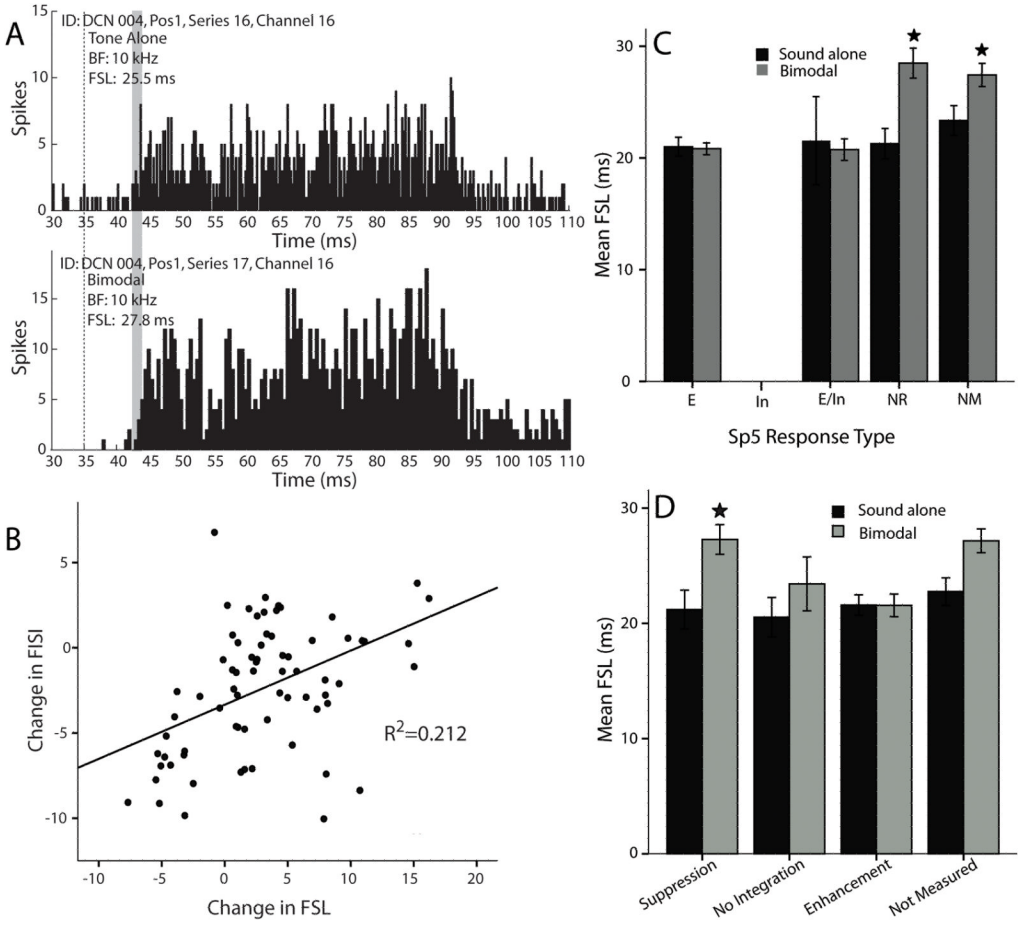

Figure 7.

Acoustic response latencies increase with Sp5 stimulation. A. PSTH of unimodal acoustic response (Top) and PSTH of bimodal response to BF tones preceded by Sp5 stimulation (Bottom), 200 Trials. Bin width = 1 ms. Dashed vertical line indicates onset of sound. Shaded vertical line highlights the increase in latency in the bimodal response. B. The change in FISI is correlated with the change in FSL. C. Mean acoustic FSLs are shown for groups of neurons with the same unimodal response to Sp5 stimulation: Bimodal FSLs (dark) are longer than unimodal acoustic FSLs (light) for NR and NM groups. E=excitation; In=inhibition; E/In=mixed; NR=no response to Sp5 stimulation; NM=Response to Sp5 stimulation not measured; Star indicates $p < 0.01$. D. Average FSLs within groups of neurons with the same type of rate integration (Suppression, Enhancement, or No Integration) are shown. FSL is significantly longer in units with bimodal suppression. Bimodal FSLs (dark); sound alone FSLs (light).

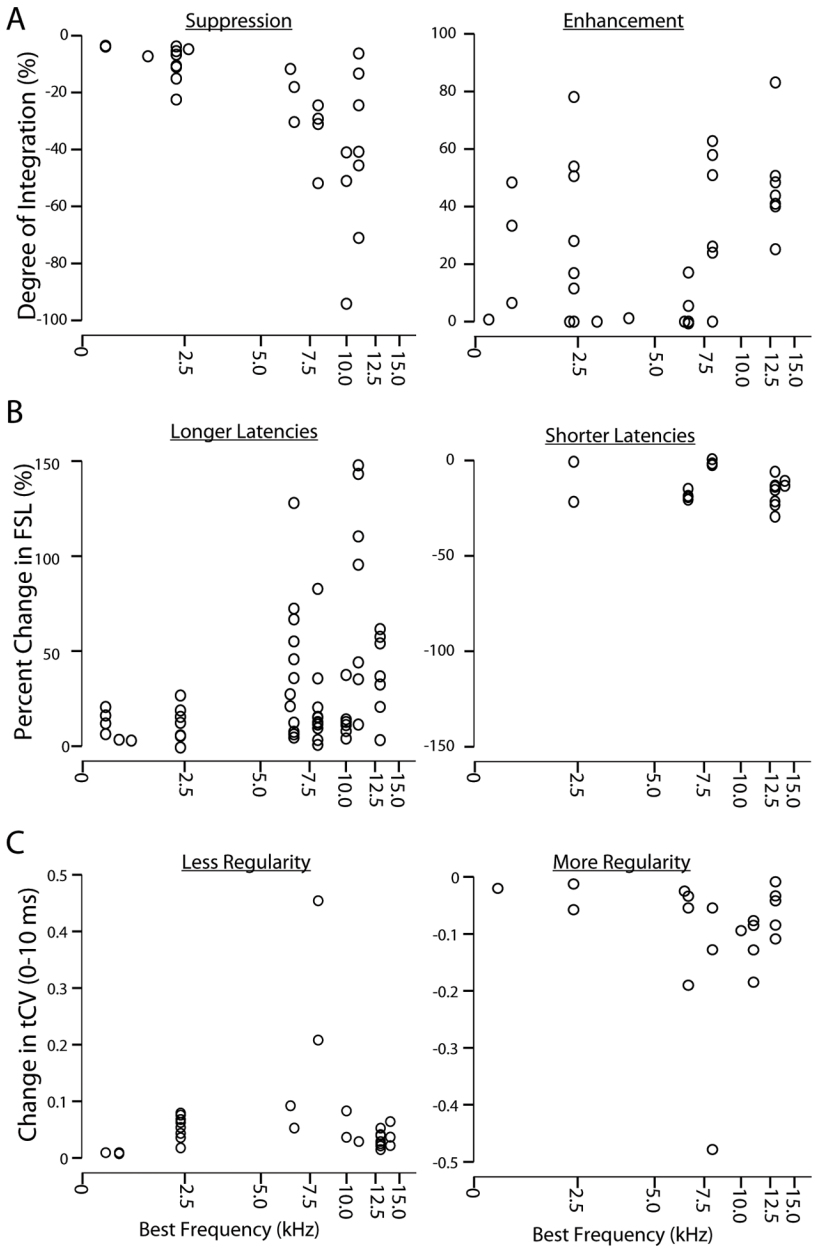

Figure 8.

Sp5-induced changes in acoustic responses are tonotopically organized. A. For each unit, the degree of suppression (left) or enhancement (right) is plotted against the best frequency of the unit. B. For each unit, the percent increase (left) or decrease (right) in latency is plotted against the best frequency of the unit. C. For each unit, the increase (left), or decrease (right) in transient CV is plotted against the best frequency of the unit.